Minerals Engineering 43–44 (2013) 12–21

Contents lists available at SciVerse ScienceDirect

Minerals Engineering

journal homepage: www.elsevier.com/locate/mineng

Multi-component AG/SAG mill model

M.P. Bueno *, T. Kojovic, M.S. Powell, F. Shi

Julius Kruttschnitt Mineral Research Centre, 40 Isles Road, Indooroopilly, QLD 4068, Australia

ARTICLE INFO

Article history:
Available online 31 July 2012

Keywords:
Autogenous grinding
SAG milling
Modelling
Multi-component ore
Blending
Mixture

ABSTRACT

The JKMRC has been studying and modelling industrial AG and SAG mills for over 40 years, but the ability to simulate the effects of blending hard and soft components on mill performance remains quite limited. In an effort to quantify these effects for modelling purposes, a series of laboratory, pilot scale and full scale tests, using multi-component feeds were conducted under the AMIRA P9O project.

The obtained data shows a non-linear trend between the measured mill throughput and the proportion of soft component in the feed, as well as the effect of fresh feed composition in mill product size distribution and load. Therefore, a new multi-component AG/SAG mill model structure was developed to account for these observed effects, and it was validated using pilot and full scale data.

1. Introduction

The Run-of-mine composition strongly affects autogenous mill operation. However, the effects of a varying ratio of hard and soft components in mill performance are not described by the current generation of AG/SAG models (Stange, 1996). For example, current JKSimMet models (Napier-Munn et al., 1996) assume a uniform feed, and describe it using a single set of average ore breakage function parameters (A, b and t_a). JKTech (1998) has found that the simple use of weighted average parameters may generate a significant bias in the simulated mill performance, as it does not consider the specific characteristics of different ore types (e.g. competence, toughness and abrasion resistance) as measured by standard ore characterisation parameters such as JK $A*b$ values and the Bond work index (Wi).

The hard component typically limits the mill throughput, due to its slower breakdown characteristics, and preferentially accumulates in the mill contents; impacting the mill power when these components have different specific densities. Competent materials also affect the product size distribution because they comminute predominantly by abrasion and generate more fines, while soft or brittle materials produce a coarser product. Therefore, there is a clear need to quantify the behaviour of binary feeds in AG/SAG mill operations and to develop a multi-component model structure.

The grinding media of autogenous mills derive from the feed ore size and composition (Delboni and Morrell, 1996) and the varying ratio of different components in the mill feed affects the mill charge and consequently the whole breakage process. after developing a new AG/SAG mill model that describes the influence of mill charge composition on breakage performance, Delboni (1999) recommended investigating multi-component ore interactions in order to develop a model structure that accounts for preferential accumulation of hard ore types in the mill load. However, this well known effect has rarely been quantified or modelled.

A comprehensive experimental campaign was conduct with the AMIRA P9O project to understand the behaviour of multi-component ores in AG/SAG mills (Bueno et al., 2010, 2011a, 2011b). The results were then used in the development of a 2D phenomenological model described in this paper.

2. JKSimMet AG/SAG model overview

The AG/SAG Model in the JKSimMet simulation package is based on a framework developed by Leung (1987), shown in Fig. 1. This model structure is briefly described in this section and was used as a platform to develop the multi-component model presented in this paper.

2.1. Size reduction and throughput

As shown in Fig. 2, the size reduction processes inside an AG/SAG mill, when in steady state, are encapsulated by the perfect mixing model (Whiten, 1974) equations:

$$f - R \cdot s + A \cdot R \cdot s - D \cdot s = 0 \quad (1)$$

$$p = D \cdot s \quad (2)$$

where f is the feed rate, p the product rate, R = breakage rate, s the mill contents, D the discharge function and A is the appearance or breakage distribution function

* Corresponding author. Tel.: +61 7 3346 5983, Mobile: +61 4 1324 9712; fax: +61 7 3365 5999.
E-mail address: m.bueno@uq.edu.au (M.P. Bueno).

0892-6875/$ - see front matter © 2012 Elsevier Ltd. All rights reserved.
http://dx.doi.org/10.1016/j.mineng.2012.06.011

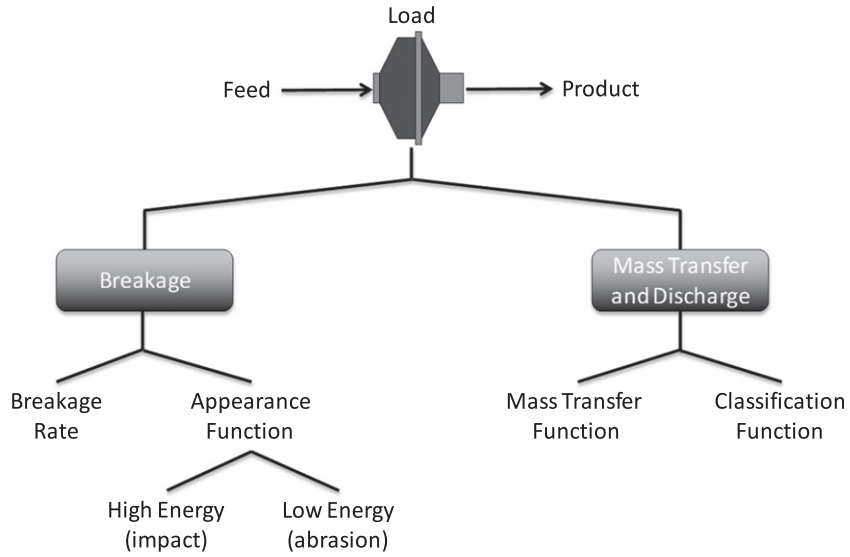

Fig. 1. AG/SAG Model Structure after (Leung, 1987).

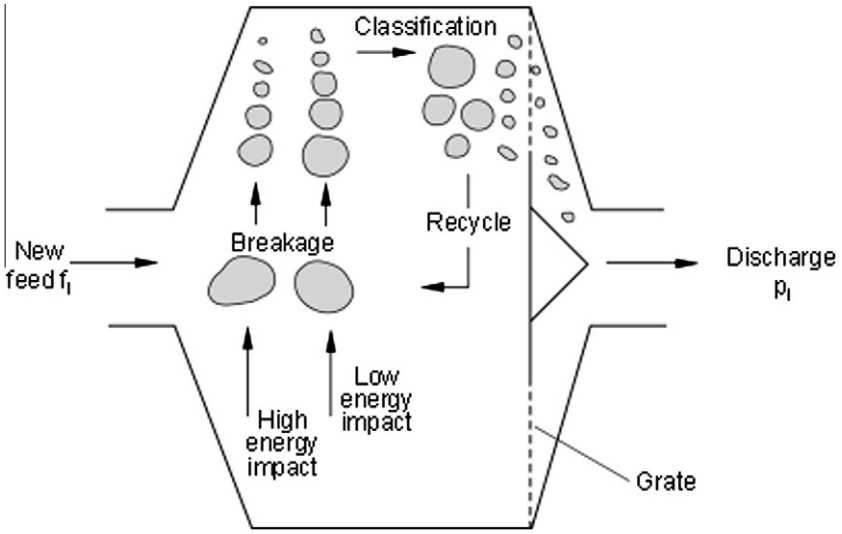

Fig. 2. Schematic diagram of AG/SAG mill process mechanisms after (Napier-Munn et al., 1996).

2.2. Mass transfer and discharge

The mill discharge rate for each particle size is a product of the maximum discharge rate through the grate (h^{-1}), multiplied by the grate classification function for each size. This is modelled using the following equation:

$$d_i = D_{max} \cdot c_i \quad (3)$$

where d_i is the discharge rate of size class i, c_i the classification function value for size class i, D_{max} is the maximum discharge rate (h^{-1}).

The grate classification function (c_i) has a simple shape, characterised by two or three distinct regions, as shown in Fig. 3.

Particles up to size X_m presented to the grate will always pass through it, X_g is the grate aperture and X_p is the pebble port size and f_p is the pebble ports fraction of total open area.

The fraction of the load presented to the grate per unit of time (D) is found iteratively, in order to satisfy the following empirical relationship that relates the holdup of slurry to the total volumetric discharge (Austin et al., 1977):

$$L = m_1 F^{m_2}$$

where $m_1 m_2$ is the constants, L the fraction of mill occupied by below grate size material, F is the volumetric discharge rate, in mill fills per minute.

2.3. Appearance function

The appearance or breakage distribution function describes the progeny size distribution from each breakage event. According to Leung (1987), this function explains the breakage in terms of high (impact) and low energy (chipping/abrasion) breakage.

The high energy breakage is ore specific and related to the breakage energy, and is defined by the equation below:

$$t_{10} = A(1 - e^{-b.Ecs}) \quad (4)$$

where A and b are ore specific parameters obtained from the JK Drop Weight Tests (DWT), Ecs is the specific comminution energy and t_{10} is the progeny percent passing one tenth of the initial particle size. The t_{10} is used to generate a full size distribution using cubic splines (Narayanan and Whiten, 1988).

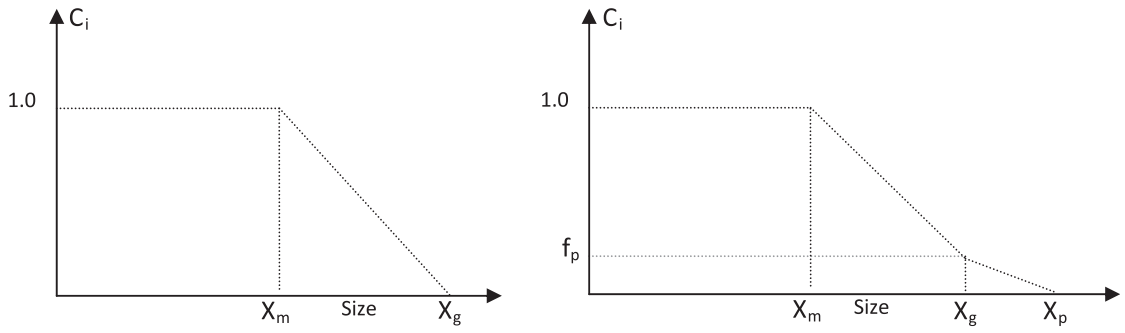

Fig. 3. Mill grate classification function (Napier-Munn et al., 1996).

The model calculates the specific comminution energy (Ecs) for each size fraction in the mill load using the highest energy reference level (E_1), which is related to the average size of the coarsest 20% of the rock charge by mass (S_{20}), and the relationship proposed by Austin et al. (1984) in Eq. (8). This is represented in the model as follows:

$$S_{20} = (p_{100} * p_{98} * p_{96} \ldots p_{80})^{1/11} \quad (5)$$

$$E_1 = 4/3\pi(S_{20})^3 \rho\, g\, D \quad (6)$$

$$\mathrm{Ecs}(1) = E_1/(4/3\pi(X_1)^3\rho) \quad (7)$$

$$\mathrm{Ecs}(i) = \mathrm{Ecs}(1)/(x_i/x_1)^{1.5} \quad (8)$$

where D is the mill diameter in metres, ρ is the ore density and Ecs (1) is the specific comminution energy for the top size (X_1). The calculated Ecs values are then used in Eq. (4) to obtain a t_{10} for each size fraction.

The low energy breakage function is also ore specific and defined by a single parameter t_a, obtained from a mill tumbling test carried out in combination with the JKDWT. The value of t_a is assumed to be the same for all size fractions and is used to define the abrasion progeny, which is similar for various ores tested to date.

The high and low appearance functions are combined proportionally, using the following relationship, which implies that abrasion will dominate for coarse particles and impact breakage for fines.

$$a = \frac{t_{LE} * a_{LE} + t_{HE} * a_{HE}}{t_{LE} + t_{HE}} \quad (9)$$

where a_{LE} and a_{HE} are the low and high energy appearance functions and t_{LE} and t_{HE} are the low and high energy t values.

2.4. Breakage rate

The breakage rates can be back-calculated using Eqs. (1) and (2), given the feed and product size distributions and flowrates, the rock load distribution and mass, as well as the measured breakage function. Cubic splines at five knots (R1–R5) are used to describe the breakage rate distribution function, which is related to particle size and usually takes the form shown in Fig. 4.

The breakage rate distributions are affected by a number of operating conditions. Morrell and Morrison (1996) modelled the effect of ball charge, mill filling, feed size distribution and mill speed on each breakage rate. The resulting 5 empirical equations are embedded in the current JKSimMet Variable Rates AG/SAG model. However, there are other elements (e.g. lifter profile and mill feed composition) which might influence these rates and are not accounted for in the current JKSimMet model.

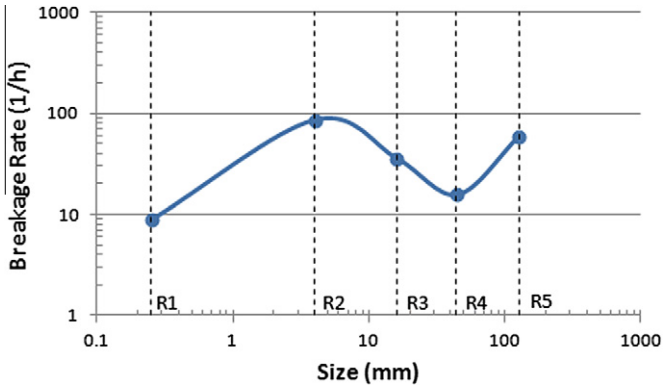

Fig. 4. Typical AG/SAG breakage rate function.

3. Multi-component model upgrades

The proposed multi-component AG/SAG mill model is similar to, and based on, the current JKSimMet model. In the new version, the behaviour of each component is described using a separate perfect mixing model equation (see Fig. 5). The major features of this model are listed below:

- More accurate calculation of specific comminution energy (Ecs).
- Independent breakage functions (A, b and t_a) for each component.
- Independent breakage and discharge rates for each component.
- Accounts for the effect of blending in the mill power draw calculation.

According to the preliminary modelling findings, the breakage rates for each component vary according to their proportion in the mill fresh feed. The reason behind this variation is that different feed blends result in different compositions in the mill charge, which act as grinding media. Therefore, the model must determine the correct steady-state ratio between hard and soft components in the mill load, in order to provide realistic breakage simulations.

3.1. Appearance function

Independent breakage function parameters (A, b and t_a) are used for each ore component. These are obtained using the same standard characterization procedures (i.e. JKDWT or JKRBT). However, the mill feed ore samples to be tested need to be carefully sorted into their different components. Many sorting techniques can be used for this purpose, depending on which characteristic is more appropriate for distinguishing and separating them (e.g. colour, density or magnetic properties). In cases where there is no correlation between rock competency and physical properties,

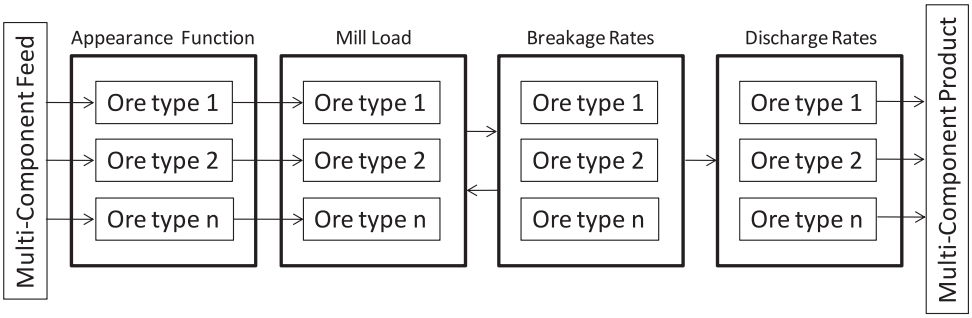

Fig. 5. Multi-Component AG/SAG mill model structure.

the selection is likely to be more difficult and should be conducted in a joint effort between geologists, mine engineers and metallurgists.

The energy calculation in the new model was refined by using the specific gravity values of each component as well as their distribution and proportion in the mill load. The bulk SG in the mill load, and the coarsest 20% size (S_{20}) is used to calculate the average energy level (E_1), which is considered to be the same for all components in the mill. Then the SG of each component is used in Eq. (7) to obtain the Ecs for each size, which is then scaled using the same relationship shown in Eq. (8). In this way, the t_{10} values are calculated using Eqs (4) and (9), with distinct specific energies and ore property parameters (A, b and t_a) inputs. This is a more realistic way of describing the breakage for each ore type in the mill, and has contributed significantly to the model integrity.

3.2. Transport and discharge rates

Multi-component experimental data (Bueno et al., 2011a) has suggested that the maximum discharge rates (D_{max}) and X_m parameters may be different for each component, due to the effects of rock density and shape. The chart in Fig. 6 shows that silicate has a higher discharge rate then magnetite.

The new model uses the same iterative method adopted by Leung (1987) and described in Section 2.2 to find the D_{max} for the bulk material. However, the D_{max} is scaled for each component after each iteration, as shown in Fig. 7.

The scale factors applied for D_{max} and X_m aim to account for a differential behaviour in transport and discharge. At this stage, they can be either fitted or calculated using experimental data when available. Further work is being conducted to model this effect according to the volumetric flowrate, the proportions of components, and the differences in specific gravity.

The current discharge model is under review, but the implications of this simplification appear to be small given the validation presented later in this paper. However, the most recent advances in slurry transport research (Latchireddi, 2002) will be implemented to account for the effects of grate design, mill speed, charge volume and pulp lifters.

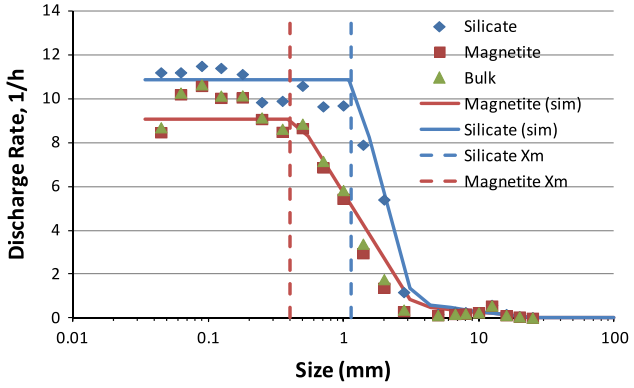

Fig. 6. LKAB pilot mill discharge function (experimental and simulated).

3.3. Breakage rates

Breakage rates have been a controversial topic of discussion between researchers given their differing interpretations of what constitutes a breakage event. Rather than considering it as the rate of breakage events occurring to each particle per unit of time (Morrell, 1989), it can be simply interpreted as being the mass transfer rate (1/h) from coarse to smaller size fractions, once the perfect mixing model is a mass balance equation. However, the breakage rate is dependent on the appearance function used (Leung, 1987), which is a function of the ore competency as measured by the JKDWT (or JKRBT). As this is a machine-ore interaction parameter, different components would be expected to have distinct breakage rates under the same operating conditions. The new model allows the calculation of component specific breakage rates and, when applied to experimental pilot plant data, has confirmed this hypothesis. For example, the breakage rate curves for magnetite and silica shown in Fig. 8 suggest a systematic difference below 10 mm and a marked shift around 50 mm. This example will be discussed in more detailed in Section 4.1.

3.4. Mill power

The same mill power draw model, present in the current version of JKSimMet (Morrell, 1992), was adopted in the multi-component model. Morrell's power model assumes the mill charge shape as shown in Fig. 9, and the mill gross power draw to have two components: net power and no-load power.

By integrating between the limits θ_s and θ_t and between r_i and r_m, the net power (P_{net}) is given by:

$$P_{net} = 2\pi\, g\, L\, \rho \int_{r_i}^{r_m} \int_{\theta_r}^{\theta_s} N_r r^2 \cos\theta \, d\theta \cdot dr \qquad (10)$$

The no-load power draw is given by the empirical relationship below:

$$\text{No Load Power(kW)} = 3.345 (D^3\, L\, N_m)^{0.861} \qquad (11)$$

where D is the mill diameter (m), L the mill length (m), N_m the mill rotation rate (revs/s), N_r the rotation rate at radial distance r (revs/s), r_m the mill radius, r_i the charge surface radius, θ_s the angular position of the shoulder, θ_t the angular position of the toe, ρ is the charge density.

It is clear that the net power draw calculation using this model is affected by the charge density, which is directly related to ore specific gravity. The current JKSimMet model does not account

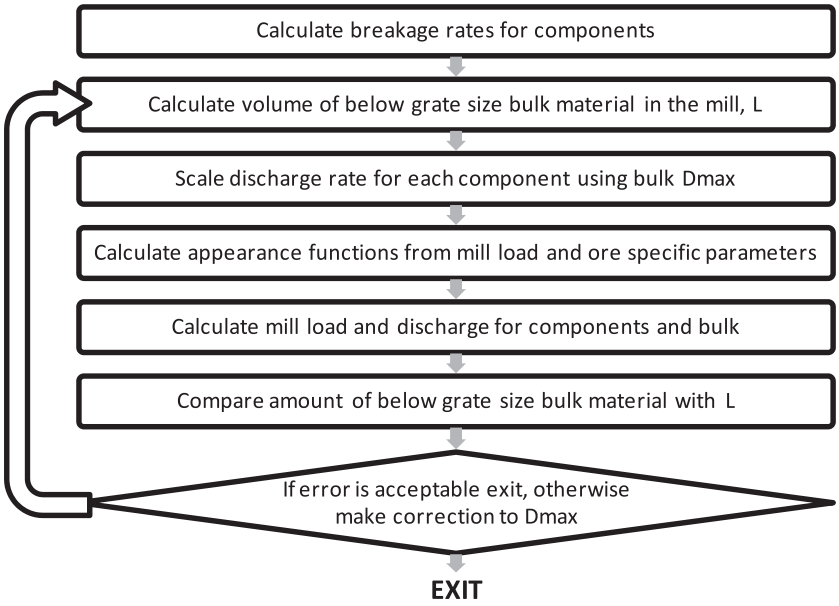

Fig. 7. Multi-component model iteration method.

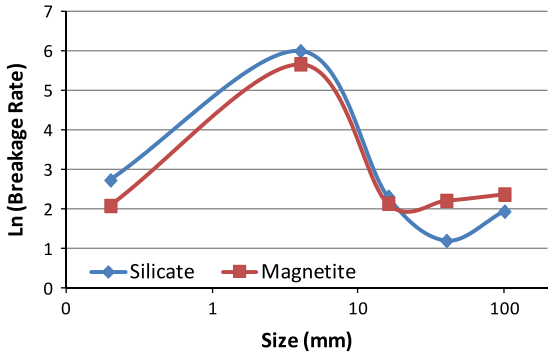

Fig. 8. Magnetite and silicate breakage rates, fitted to LKAB pilot plant data.

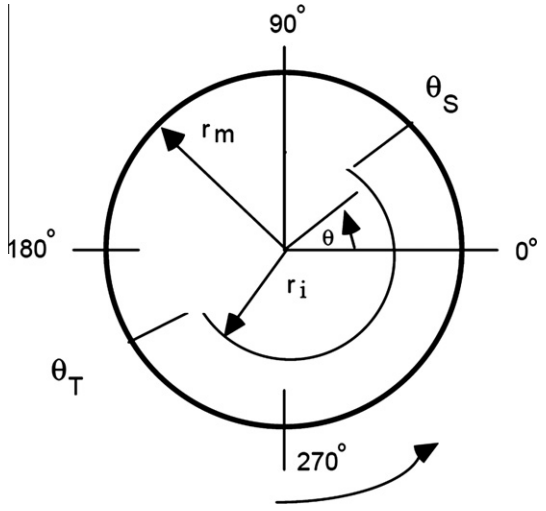

Fig. 9. Simplified AG/SAG mill charge shape (Napier-Munn et al., 1996).

for the build-up of hard components in the mill contents, and therefore, considers the ore specific gravity in the mill load to be the same as in the feed. This can lead to significant errors when hard and soft components have significant differences in specific gravity. For example, in the LKAB operation treating magnetite and silicates, the difference between the feed blend and charge density could be as high as 15% depending on the blend. This translates to a 10% difference in mill power draw.

The new model can describe very well the build-up effect, providing more realistic estimations of the true charge density, based on the balance between components and their respective specific gravities. Therefore, the effect of blending on mill power draw can now be described with more accuracy than has previously been possible.

4. Case study – model validation

Multi-component data obtained during surveys at the LKAB Kiruna concentrator in Sweden and a related pilot plant campaign using mixtures of LKAB magnetite ore and silicate waste (Bueno et al., 2011a) were used to develop and validate the proposed multi-component model.

The ore deposit in Kiruna is composed of a single continuous high grade magnetite orebody, mined using a sublevel caving method, which inevitably leads to some dilution with gangue – typically hard rock textures of silicates associated with phosphates and magnesium oxides. The mined ore has a high percentage of magnetite and is further upgraded in a sorting plant (using magnetic separation techniques) before entering the mill concentrator.

The characterization results from JKDWT (Napier-Munn et al., 1996), Bond (1952) ball mill grinding tests, density measurements and XRF assays conducted on each component are presented in Table 1.

4.1. Pilot plant

The mill was operated in fully autogenous mode and open circuit configuration during all trials. Table 2 shows the five different ratios of hard to soft (waste/magnetite) components in the mill feed trialled during this campaign. The ratio of hard to soft was changed through progressive additions of hard silicates in the +30 mm size fractions. An additional test (test T5) was carried out using an upgraded +30 mm magnetite ore, passed through a magnetic separation rig to reduce the silicate content.

Table 1
LKAB magnetite and silicate characterization results.

Measured parameter	Magnetite	Silicate
SG (t/m^3)	4.9	2.6
DWT, A	68.4	68.7
DWT, b	1.67	0.66
DWT, $A * b$	114	45.3
Abrasion, t_a	0.59	0.13
BBMWi@75 μm	13.2	15.8
XRF% Magnetite	95.7	4.3
Ore characteristic	Soft	Hard

Table 2
Mill feed composition during LKAB pilot trials.

Test	+30 mm Waste (%)	+30 mm LKAB ore (%)	−30 mm LKAB ore (%)
T1	0	30	70
T2	4	26	70
T3	8	22	70
T4	15	15	70
T5[a]	0	30	70

[a] Upgraded +30 mm ore.

The operational philosophy adopted in the pilot plant trials was to find the feed rate which resulted in a steady operation at a mill load level of 28%. Once steady-state conditions were reached, samples of feed, charge and product were collected and then analysed for size and composition distributions.

Experimental data from three trials (T1, T4 and T5), where the entire mill contents were measured, were used to calibrate the model. A total of six parameters were fitted for each component: fine size (X_m), ln(breakage rates) at knots 1–5 (R1, R2, R3, R4 and R5). The scale factors for maximum discharge rates (Dmax) were determined according to experimental data.

The calculated breakage rates for both components were affected by the feed composition, as shown in Fig. 10. This was expected because the grinding charge size and composition varied with the feed blend.

The silicate breakage rates at coarse sizes were lower than magnetite in all three trials, explaining the build-up of hard material in the mill. However, the opposite effect was observed at smaller sizes, where at the same energy levels, light silicate particles experience higher levels of specific energy (kW h/t) than dense magnetite.

The breakage rates of silicate at small sizes were not greatly affected by changes in feed blend, but magnetite breakage rates were reduced, due to a reduced level of energy provided by the less dense silicate dominated grinding media. The breakage rates were suppressed near the critical size (44 mm) for both materials. The silica breakage rates in the coarse sizes also decreased as the charge built up with more light silicate rocks (T4). The high breakage rate for silicate rocks in T5 is suspected to be an artefact of the model fitting since there would have been few silicate rocks in the +30 mm fraction of the upgraded feed. However, the magnetite breakage rates at coarser sizes increased from Test 1 to Test 5.

The effect of blend on breakage rates requires further investigation, and the new multi-component model is an ideal platform for this investigation. Meanwhile, the current model can still be used for simulation, once the effect of blend on breakage rates is measured using a few sets of pilot data.

Alternatively, data from a recently developed SAG Locked Cycle Test (Bueno et al., 2010) may be used to model the effect of feed blend. This is currently under investigation. The SAG Locked Cycle Test has been shown to reproduce the pilot mill throughput response and the load composition of both pilot and industrial mills for a given blend (Bueno et al., 2011a).

4.1.1. Modelling outcomes

Once calibrated, the multi-component model can reproduce the multi-component experimental data. A comparison between measured and simulated data for product and mill load in Test 1 is shown in Table 3 and Fig. 11. The same quality of fit was obtained for other blends treated in Tests 4 and 5.

It is clear from Table 4 that the multi-component model was also successful in simulating the build-up of hard silicate within the mill contents, which is an important effect that has implications in every other outcome of the simulation, including the mill power draw. The accuracy was also excellent when describing this phenomenon in terms of size-by-size composition, as shown in Fig. 12 for Test 1.

Ultimately, the model was able to describe very well the mill load and product size distributions for magnetite, silicate and bulk material for all trials. Fig. 13 illustrates the predictions for Test 1.

Table 3
Experimental and simulated data for test 1.

	Product		Load	
	Exp	Sim	Exp	Sim
Solids (tph)	1.86	1.86	1.95	2.03
% Solids	75.30	75.30	95.00	96.61
Liquid (tph)	0.61	0.61	0.10	0.07
Solids SG (t/m^3)	4.48	4.45	4.04	4.06
Pulp SG (t/m^3)	2.41	2.41	3.51	3.68
Volumetric flowrate (m^3/h)	1.03	1.03	0.55	0.52
% Passing 0.045 mm	47.0	52.3	4.3	5.1
80% Passing size (mm)	0.122	0.130	69.73	67.95

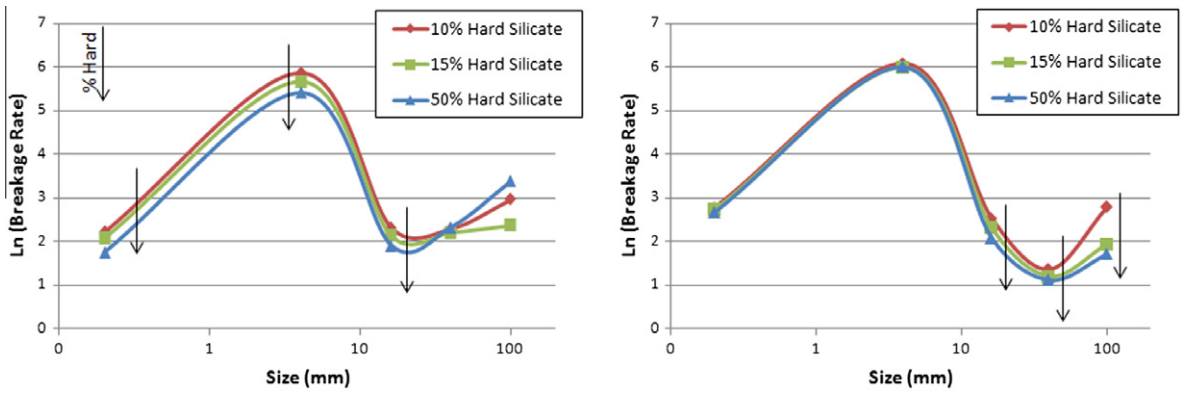

Fig. 10. Effect of feed blend on magnetite and silicate breakage rates.

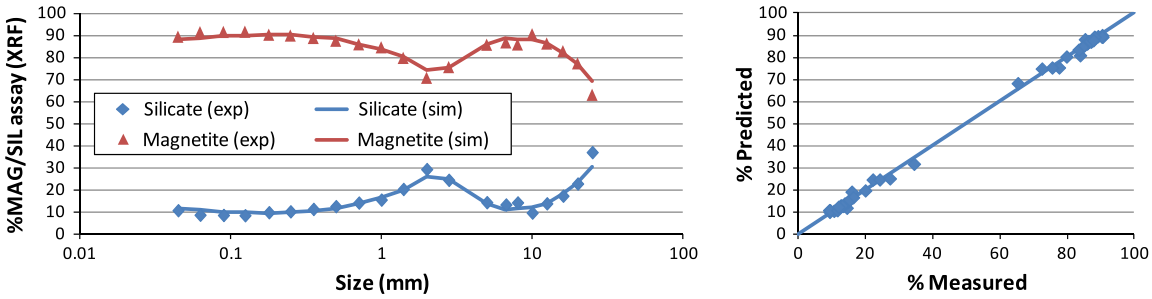

Fig. 11. Predicted and measured mill discharge assay-by-size data for Test 1.

Table 4
Build-up of hard component (exp vs. sim).

Test	% Hard silicate					
	Feed	Load		Feed +30 mm	Load +30 mm	
		Exp	Sim		Exp	Sim
T1	13.3	24.9	25.3	14.6	31.7	30.9
T4	27.9	69.4	68.1	53.1	83.8	84.2
T5	11.4	17.5	16.9	10	20.6	20.1

4.1.2. Simulation – model predictions

The variation in breakage rates according to blend, shown in Fig. 10, was modelled off-line allowing for the simulation of different feed blend conditions. The aim of this exercise was to verify the multi-component model response to blend, in terms of mill throughput, product size, energy consumption and mill load composition. The simulation procedure followed the operating protocol adopted during the pilot campaign. Therefore, the simulation was run for the average LKAB ore as is, and then for increasing increments of hard waste in the +30 mm feed. Additionally, three upgraded +30 mm feeds were simulated, one at the same upgraded magnetite grade as piloted and the other two, at higher and lower magnetic separation efficiencies. The simulation outcomes and the various model responses to blends are illustrated in Fig. 14, where the dashed line represents the average grade LKAB ore results.

The simulation results were very realistic, describing well known and expected effects such as:

- non-linear mill throughput response,
- linear relationship between specific energy and feed blend,
- increase in the amount of fines with more competent material, which is ground predominantly by abrasion, and
- build-up of hard material in the mill load.

The modelling outcomes were also in strong agreement with the measured data. The only exception was the mill product size, which was coarser (P80) but at a marginally higher percentage passing 45 μm.

4.2. Application of new model to Kiruna concentrator AG mill

The LKAB KA2 concentrator in Kiruna was surveyed to obtain detailed multi-component data for every stream and mill load (Bueno et al., 2011a). Every sample collected during this campaign was analysed for percent solids, size distribution and assay-by-size (XRF). The data was used in this study to evaluate the new multi-component model's (2D) ability to describe an industrial mill operation, as well as to compare the simulation outcomes against the current JKSimMet AG/SAG model (1D).

The models were almost equivalent when applied to the bulk data. The new model was more accurate when predicting the mill product and load size distributions, but the original model was marginally more accurate in predicting the amount of fines in the mill load, as shown in Table 5.

The extra value added by the new model became evident when it demonstrated the ability to simulate the distributions of magnetite and silicate in both the mill load and product, while the original model was limited to bulk data, as shown in Fig. 15.

The product size distribution for different phases is an excellent feature to use in assessing the impact of mill product on downstream processes, such as classifiers, magnetic separators and secondary milling. However, multi-component models for other processing units are required for a complete flowsheet simulation. This is an objective for future research within the JKMRC and AMIRA P9P project.

Another valuable feature of the new model structure is the ability to describe the build-up of hard component material in the mill load. The simulated amount of hard silicate against measured data is presented in Table 6 and Fig. 16 on a size-by-size basis.

In the case of the LKAB ore, where hard and soft components have significant differences in SG, the ability to predict the mill load composition, and consequently the charge density, will have a significant impact on mill power calculations and throughput.

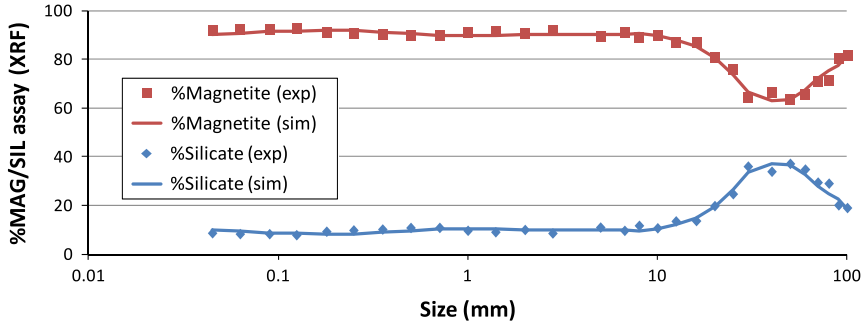

Fig. 12. Predicted and measured load composition size-by-size for Test 1.

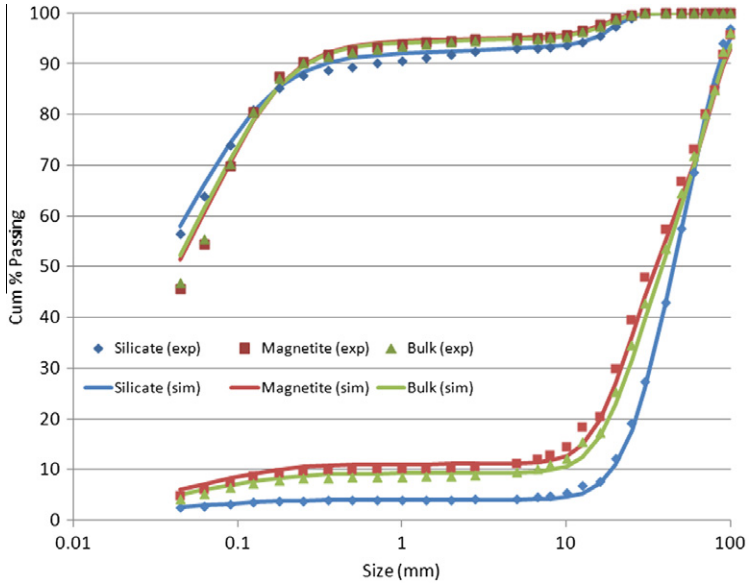

Fig. 13. Mill load and product size distributions (exp vs. sim) for Test.

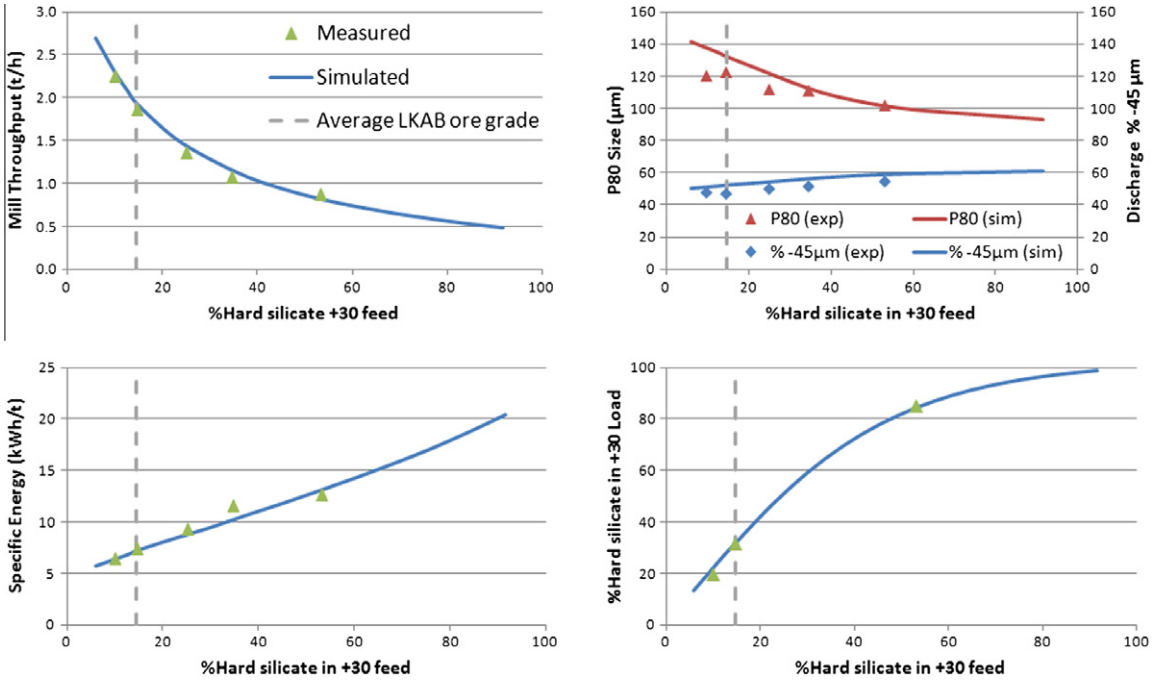

Fig. 14. Simulation outcomes and model response to feed blend.

Table 5
Comparison of experimental data and simulation results for KA2 AG mill using 1D and 2D models.

	Product			Load		
	Exp	Sim 1D	Sim 2D	Exp	Sim 1D	Sim 2D
Solids (tph)	453	453	453	155	168	159
% Passing 0.045 mm	25.2	30.1	28.0	4.8	4.5	4.2
80% Passing size (mm)	0.430	0.615	0.520	72.5	84.9	77.9

Table 7 shows the mill power calculations for both the 1D and 2D models. The new model predictions are more accurate because they account for a larger amount of light silicate in the mill load (i.e. lower total charge density, t/m^3).

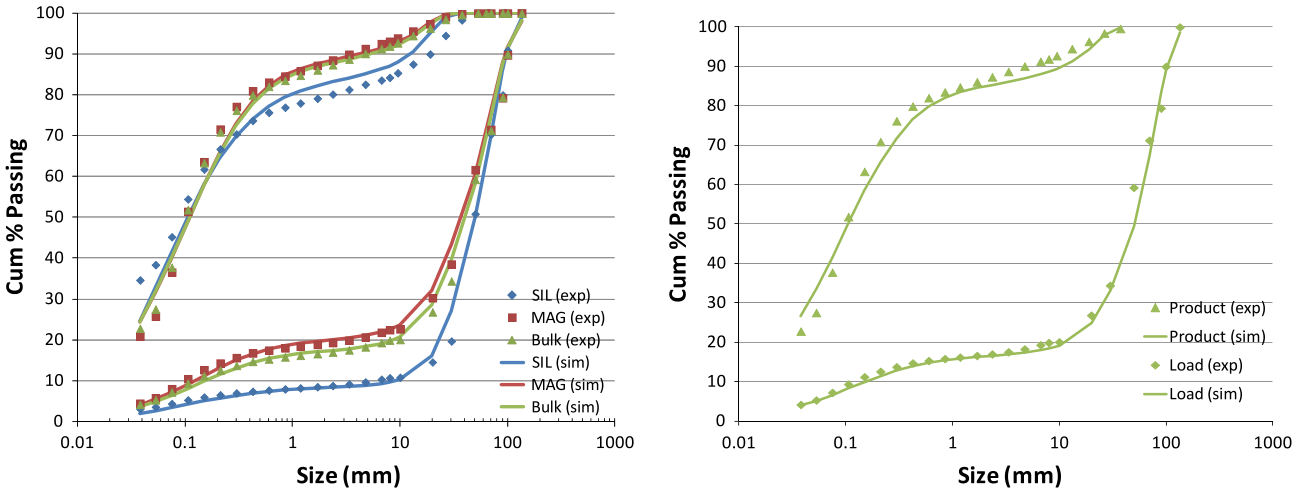

Fig. 15. Comparison of product and Load size distributions for 2D vs. 1D models.

Table 6
% Hard Silicate in KA2 AG mill feed and load (exp vs. sim).

% Hard silicate					
Feed	Load		Feed +30 mm	Load +30 mm	
	Exp	Sim		Exp	Sim
13.3	22.0	22.9	14.8	24.5	25.9

Table 7
Mill power calculations (1D, 2D and measured).

	1D	2D	Meas.
% Volumetric total load	30.3	30.8	30.5
Total charge density (t/m^3)	3.6	3.3	–
Net power (kW)	2176	2020	–
No load power (kW)	319	319	–
Gross power (kW)	2961	2772	2767

5. Conclusions

By upgrading the current JKSimMet 1D model structure to a 2D data format, allowing for the specification of the feed on a component by size basis, a new simple and robust multi-component model has been developed. The model relies on independent breakage and discharge rates for each component, and when combined still observe the underlying discharge rate of the bulk solids and water.

The model was refined and validated using multi-component data obtained through pilot tests and an industrial mill survey at LKAB in Sweden.

It has been shown that the model is capable of correctly describing the changes in throughput capacity, mill load and product caused by changes in the mill feed composition.

Further work is being carried out to implement the most recent advances in the fields of breakage energy calculation and slurry transport, as well as to model the effect of changes in feed blend on the mill breakage rates.

Although the case studies presented were all AG related, the model is applicable to SAG mills and uses the same method as the previous JKSimMet model to account for the extra energy provided by steel balls.

The model should find applications in the optimization of existing circuit operations with multi-component ores, and in the field of geometallurgical mine-to-mill optimization exercises. When other multi-component models are available (e.g. classifiers, HPGR and ball mill), it can be used to assess flowsheet alternatives to optimise the grinding performance specific to each ore component.

Acknowledgements

This study was made possible through the Julius Kruttschnitt Mineral Research Centre and supported by the AMIRA P9O Project. The authors wish to acknowledge the extensive financial and logistical support from LKAB and all the staff involved in obtaining the data presented in this paper. Special thanks are due to Michal Andrusiewicz, JKTech's lead programmer who has made significant contributions towards programming this model in the JK MDK platform.

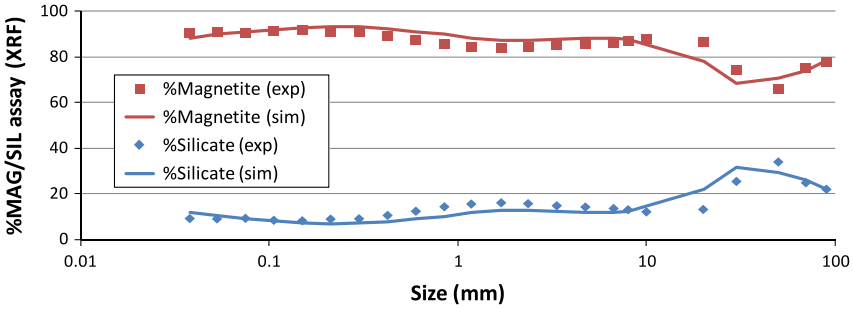

Fig. 16. KA2 mill load composition (exp vs. sim).

References

Austin, L.G., Weymont, N.P., Prisbrey, K.A., Hoover, M., 1977. Preliminary results on the modeling of autogenous grinding. In: Ramani, R.V. (Ed.), APCOM 76: Proceedings of the Fourteenth International Symposium on the Application of Computers and Mathematics in the Mineral Industry, AIME, Soc. Min. Eng., University Park, PA, USA, pp. 207–226.

Bond, F.C., 1952. Third theory of comminution. Mining Engineering 4 (5), 484–494.

Bueno, M., Neva, E., Powell, M.S., Fredriksson, A., Kojovic, T., Worth, J., Shi, F., Adolfsson, G., Partapuoli, Å., Wikström, P., Olofsson, M., Tano, K., 2011a. The dominance of the competent. In: Mular, A.L., Barratt, D.J., Knight, D.A. (Eds.), Fifth International Autogenous and Semiautogenous Grinding Technology, University of British Columbia, Department of Mining and Mineral Process Engineering, Vancouver.

Bueno, M., Shi, F., Kojovic, T., Powell, M.S., 2010. Investigation on multicomponent semi-autogenous grinding. In: XXV International Mineral Processing Congress. Australasian Institute of Mining and Metallurgy, Brisbane, Australia, CD-ROM, p. 1.

Bueno, M., Shi, F., Kojovic, T., Powell, M.S., Sweet, J., Philips, D., Durant, B., Plint, N., 2011b. Multi-component autogenous pilot trials. In: Mular, A.L., Barratt, D.J., Knight, D.A. (Eds.), 5th International Autogenous and Semiautogenous Grinding Technology, University of British Columbia, Department of Mining and Mineral Process Engineering, Vancouver.

Delboni, H., 1999. A Load-interactive Model of Autogenous and Semi-Autogenous Mills. University of Queensland, Australia [St. Lucia, Qld.], p. 1v.

Delboni, H., Morrell, S., 1996. The modeling of autogenous and semiautogenous mills. In: Mular, A.L., Barratt, D.J., Knight, D.A. (Eds.), International Autogenous and Semiautogenous Grinding Technology, University of British Columbia, Department of Mining and Mineral Process Engineering, Vancouver, pp. 713–728.

JKTech, 1998. Minutes from JKSimMet Discussions. Private Communications, Private Communications Ed., Private Communications, Brisbane.

LATCHIREDDI, S. R. 2002. Modelling the performance of grates and pulp lifters in autogenous and semi-autogenous mills. Ph.D. Thesis, University of Queensland, Australia.

Leung, K., 1987. An energy based, ore specific model for autogenous and semi-autogenous grinding mills. In: JKMRC. University of Queensland, Australia, Brisbane, Australia, p. 1v.

Morrell, S., 1989. Simulations of bauxite grinding in a semi-autogenous mill and DSM screen circuit. In: JKMRC. University of Queensland, Australia [St. Lucia], p. 259 l.

Morrell, S., 1992. Prediction of grinding-mill power. Trans. Inst. Min. Metall. Sect. C-Miner. Process. Extr. Metall. 101, C25–C32.

Morrell, S., Morrison, R.D., 1996. Ag and sag mill circuit selection and design by simulation. In: Mular, A.L., Barratt, D.J., Knight, D.A. (Eds.), International Autogenous and Semiautogenous Grinding Technology. University of British Columbia, Department of Mining and Mineral Process Engineering, Vancouver, pp. 769–790.

Napier-Munn, T.J., Morrell, S., Morrison, R.D., Kojovic, T., 1996. Mineral Comminution Circuits: Their Operation and Optimisation, first ed. Julius Kruttschnitt Mineral Research Centre, Indooroopilly, Qld. (Reprinted with Minor Corrections 1999, 2005, Ed. 2005).

Narayanan, S.S., Whiten, W.J., 1988. Determination of comminution characteristics from single-particle breakage tests and its application to ball-mill scale-up. Trans. Inst. Min. Metall. Sect. C-Miner. Process. Extr. Metall. 97, C115–C124.

Stange, W., 1996. The modeling of binary ore behaviour in FAG/SAG milling. In: Mular, A.L., Barratt, D.J., Knight, D.A. (Eds.), International Autogenous and Semiautogenous Grinding Technology. University of British Columbia, Department of Mining and Mineral Process Engineering, Vancouver, pp. 1063–1080.

Whiten, W.J., 1974. A matrix theory of comminution machines. Chem. Eng. Sci. 29 (2), 589–599.